A MEMS Micro Force Sensor
for Drosophila Flight Characterization

Yu Sun[1], *Member, IEEE* , C.F. Graetzel[2], S.N. Fry[3], and B.J. Nelson[2], *Member, IEEE*
[1]*Advanced Micro and Nanosystems Laboratory, the University of Toronto*
[2]*Institute of Robotics and Intelligent Systems, Swiss Federal Institute of Technology (ETH)*
[3]*Institute of Neuroinformatics, University of Zürich*

Abstract—**This paper reports a MEMS micro force sensor with a novel configuration of differential tri-plate comb drives suitable for bulk micromachining. A high-yield fabrication process using DRIE on SOI wafers is utilized to construct the high aspect ratio devices. The sensor has a high sensitivity, good linearity, and a large bandwidth, which are required for characterizing flight behavior of fruit flies (Drosophila). The technique allows for the instantaneous measurements of flight forces, which result from a combination of aerodynamic and inertial forces generated by the wings. The potential impact of this research extends beyond gathering flight data on Drosophila melanogaster by demonstrating how MEMS technology can be used to provide valuable tools for biomechanical investigations.**

I. INTRODUCTION

AS scientists and engineers strive to develop more intelligent microrobotic systems, many in the field are increasingly turning towards biological organisms in order to provide design inspiration. For example, researchers have considered cockroaches [1] [2], crickets [3], and earthworms [4] to guide the design of small autonomous microsystems. Over the past few years, the flight behavior of small insects has attracted interest for the development of flying microrobotic systems [5]. One such insect that is particularly interesting from the standpoint of complete flight system design is the fruit fly Drosophila melanogaster.
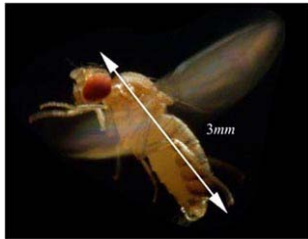

Fig. . Drosophila melanogaster in typical hovering posture.

The fruit fly, shown in Fig. 1, is a model organism studied by biologists for almost a century, and possesses a highly developed flight control system that provides them with the capability to perform robust stable flight, as well as

exceedingly rapid and precise turning maneuvers. The neurophysiology and biomechanics are inextricably linked and must be considered at the systems level. Multimodal sensory input converges on only 18 control muscles that are responsible for the fine-tuning of wing motion for maneuvering. Beyond its impressive flight behavior, the fact that Drosophila is completely autonomous, extremely small, highly robust, and self replicating makes this organism particularly interesting from a microrobotics standpoint [6].

II. CHALLENGES AND APPROACH

To better understand the biomechanics of flight behavior, precise measurements of the flight forces of these tiny (3mm long) insects must be obtained. The challenges of accomplishing this task are mainly caused by the small size of Drosophila (and subsequently the small forces involved), the frequency of the wing beat (approximately 200Hz) and the need to be as minimally invasive as possible. Apart from these measurement issues, the complexity of insect flight, from wing hinge to wake interactions, explains why it is still today an intense topic of research for biology [7].

Past approaches to studying Drosophila's flight behavior can be divided into three main categories:
1. Determining the forces from a computational fluid dynamic model [8]
2. Computing the forces from an upscaled robotic model [9]
3. Directly measuring the forces from a tethered fruit fly [10]

Approaches 1 and 2 have the advantages of being able to test various hypotheses about force generation and of estimating free flight force generation [11], but rely heavily on precise geometrical and kinematic input which are cumbersome to obtain. Modeling problems are circumvented in approach 3, although the tether induces flight behavior modifications. This final limitation is significant; however approach 3 remains the most interesting from a microrobotic perspective: closed-loop experiments, which consist in creating feedback loops in between flight forces and visual input, give a unique mean to investigate the neural sensor integration and motor control underlying complex flight behavior.

The tethered method has been previously implemented by measuring flight forces exerted by flies tethered on a steel wire. Displacements caused by the forces were measured using laser interferometry [10]. In principle, this

method is suitable for measuring the instantaneous flight forces in the fly's sagittal plane; however, measurements artifacts due to resonance issues were also reported. Although it allows detailed measurements, this method has not found broad application in biomechanical studies, possibly due to the relative complexity of the set up.

MEMS sensors provide the opportunity to develop small and inexpensive sensors that allow high sensitivity and bandwidth measurements, and hence may provide significantly enhanced data acquisition technology in many areas of biological research, such as flight dynamic studies of Drosophila. This paper presents a MEMS micro force sensor capable of precisely capturing in real time both aerodynamic forces and inertial forces. The potential impact of this research extends beyond gathering flight data on Drosophila, by demonstrating how MEMS technology can be used to provide valuable tools for biological investigations.

III. MEMS FORCE SENSING

Various MEMS force sensor designs have been proposed and realized, including piezoresistive, piezoelectric, capacitive, optical and magnetic. Capacitive microforce sensing has the advantages of low power, low noise, high sensitivity, and insensitivity to temperature variation. The common configurations are lateral comb drives (overlapping area changes) [12] and transverse comb drives (gap changes) [13]. Compared to the lateral configuration, transverse comb drives have higher sensitivity but suffer from significant nonlinearity. The comb drives described in this paper are of the transverse orientation; however, they provide both the high sensitivity and linearity that traditional transverse comb drives lack.

Differential tri-plate comb drives have been used, for example, in the ADXL50 accelerometer [14]. ADXL50's surface micromachined comb drive configuration is easily realized in surface micromachining; however, it is not suitable for production by bulk micromachining due to the difficulty of electrically isolating the two stationary capacitor plates. Because bulk micromachining is capable of constructing higher aspect ratio comb drives for improving sensitivity, two connected capacitor pairs were used in this paper to construct differential comb drives that were bulk micro-machined, which was achieved by separating the two stationary capacitor comb sets on either side of the movable comb set (Fig. 2).
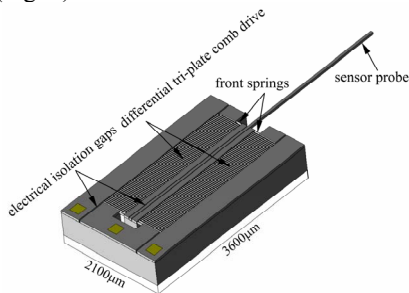

Fig. 2. Force sensor solid model

The high aspect ratio device described in this paper was constructed by a simple and high-yield fabrication process using DRIE on SOI wafers [13]. In this process, the handle layer Si substrate does not need to be patterned before fusion bonding. The handle layer is an integrative part of the force sensor, used for structural stability, dice free releasing of the fragile structures, suspending the comb capacitors, as well as mechanically connecting and electrically isolating capacitor plates, which is shown in Fig. 2.
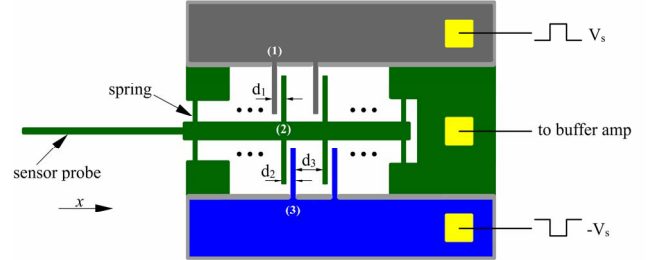

Fig. 3. Force sensor schematic

IV. MICRO FORCE SENSOR DESIGN

Fig. 2 shows the solid model of the micro force sensor design. The sensor probe transmits forces axially deflecting the unidirectionally compliant springs. This deflection displaces the inner moveable capacitor plates - plates (2) shown in Fig. 3. With a force applied in the positive x direction, plates (2) move away from plates (1) and closer to plates (3). When an AC signal is applied to the outer capacitors (plates (1) and (3)), a voltage divider is formed, as shown in Figure 4.
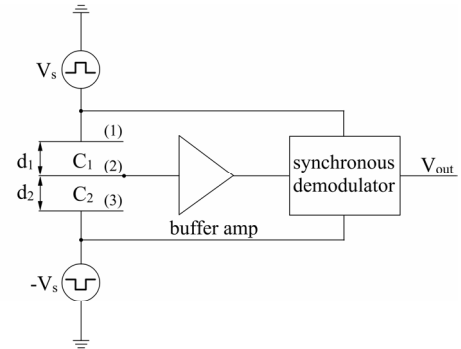

Fig. 4 Block diagram and readout circuit

The resulting signal V_{out} is

$$V_{out} = V_s \left(\frac{C_1 - C_2}{C_1 + C_2} \right) \qquad (1)$$

where $C_1 = K\varepsilon \frac{A_1}{d_1} + K\varepsilon \frac{A_1}{d_3}$, $C_2 = K\varepsilon \frac{A_2}{d_2} + K\varepsilon \frac{A_2}{d_3}$, K is the dielectric constant for the ambient (for air $K = 1$) $\varepsilon = 8.8542 \times 10^{-12} C^2 /(N \times m^2)$ is the permittivity of free space, and overlapping plate area $A_1 = A_2$. The plates are nominally spaced equally at $d_0 = (d_1 + d_2)/2$. The plate

distances are, thus, defined as $d_1 = d_0 + \Delta d$ and $d_2 = d_0 - \Delta d$, where Δd is the displacement of the middle plate. By initially setting $d_1 = d_2 << d_3$, the undesired additional parallel capacitance effect is minimized, and linearity is maintained. From (1), the resulting output signal V_{out} can be shown to be proportional to the middle plate displacement.

$$V_{out} = V_s \left(\frac{\Delta d}{d_0} \right) \qquad (2)$$

Fig. 5 shows the deflection-output relationship for $d_3 = 6, 8, 20 \mu m$ (in all cases $d_1 = d_2 = 5 \mu m$). It can be seen that repeating the comb drive unit reasonably far apart makes the undesired parallel capacitance effect negligible and maintains system linearity.
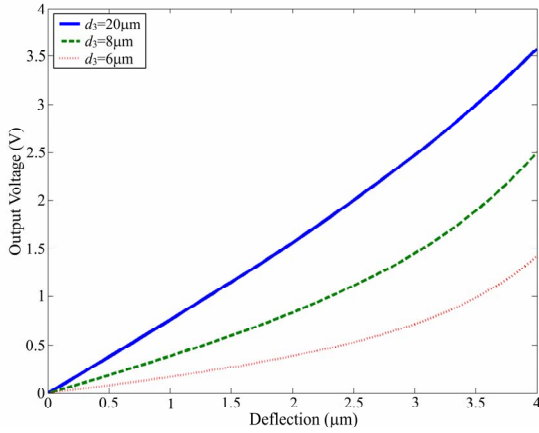

Fig. 5. Linearity comparison by varying gap d3.

The stiffness of the sensors is determined by the spring dimensions. The springs are modeled as two fixed-fixed beams with a point load applied in the middle. The force-deflection model is [15]:

$$\Delta d = \frac{FL^3}{4Ew^3 t} \qquad (3)$$

where F is the total applied force, $E = 100 GPa$ is the Young's modulus of P-type <100> silicon, and L, w, and t are spring length, width, and thickness.

V. MICROFABRICATION

Fig. 6 illustrates the microfabrication process. **Step A** to **Step D** can be replaced by directly purchasing commercial SOI wafers. After **Step E**, the wafer is fragile due to the deep trenches on the backside; however, the $50 \mu m$ top Si layer is study enough for subsequent processing from the support of the remaining Si on the handle layer.

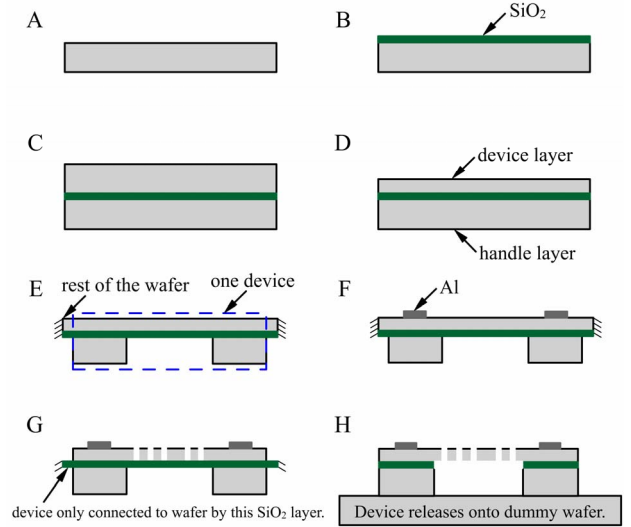Fig. 6. **Microfabrication process**

A. Start from a double polished P-type wafer with crystal orientation of <100>.

B. LPCVD (Low Pressure Chemical Vapor Deposition) 1μm SiO2.

C. Fusion bond the wafer with SiO2 with another P-type wafer.

D. CMP (Chemical Mechanical Polishing) the top wafer (the device layer) down to 50 m. This forms an SOI (silicon-on-insulator) wafer.

E. DRIE (Deep Reactive Ion Etching) to form the features on the back side (the handle layer) such as the outer frame and inner movable structure. The buried 1 m SiO2 layer acts as an etch stop layer and as an insulator between the capacitors.

F. E-beam evaporate Al to form ohmic contacts. Lift-off to pattern Al.

G. DRIE the top side to form capacitive comb fingers and springs. The devices were connected to the device wafer only by the buried SiO2 layer.

H. RIE (Reactive Ion Etching) to remove the buried SiO2 layer.

The devices were released onto a carrier dummy wafer below the device wafer, and then were picked up individually from the carrier dummy wafer. The dice-free release process protects fragile structures from damage.

In this design and process, the handle layer Si is an integrative part of the force sensor, used for structural stability, dice free releasing of the fragile structures, suspending the comb capacitors, as well as mechanically connecting and electrically isolating capacitor plates, which is shown in Fig. 2. The comb capacitor plates are 50 μm in depth, greatly increasing device sensitivity because of the large overlapping area. An aspect ratio of more than 100 can be achieved using the microfabrication process. Fig. 7 shows an SEM picture of a completed device.
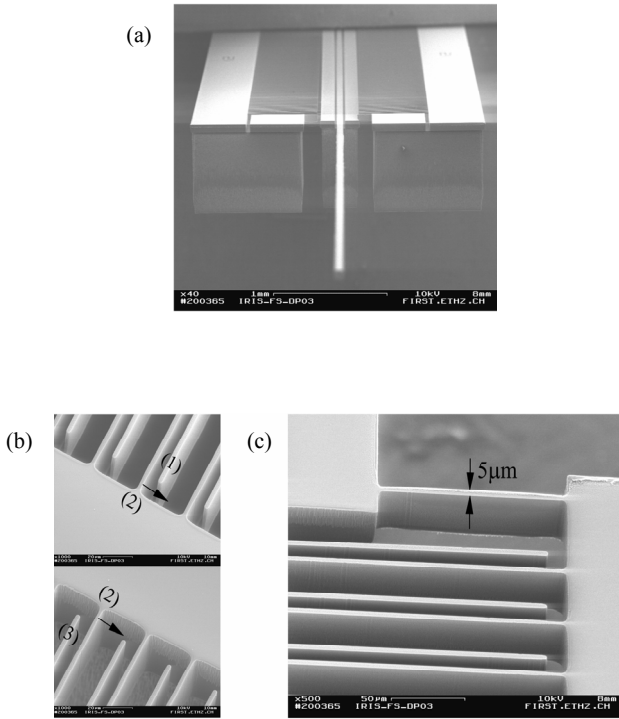
(a)

(b)

(c)

Fig. 7. (a) SEM of a force sensor.

(b) Differential tri-plate comb drives.

(c) Suspended spring and comb drives.

Table 1. Device specifications.

resolution		0.68µN
sensitivity		1.35µN/mV
range		+/- 1mN
bandwidth		7.8kHz
dimensions	base	3.6mm × 2.1mm × 0.5mm
	probe	3mm × 50µm × 50µm
	cap gap (d_1,d_2)	5µm
	cap spacing (d_3)	20µm
	cap plates	500µm × 5µm × 50µm
	springs	125µm × 5µm × 50µm

The electrostatic force generated from the excitation voltages is

$$F_e = \frac{NA\varepsilon V^2}{2} *$$

$$\left[\frac{1}{(d_0 - \Delta d)^2} - \frac{1}{(d_3 + \Delta d)^2} + \frac{1}{(d_3 - \Delta d)^2} - \frac{1}{(d_0 + \Delta d)^2} \right] \quad (4)$$

where N is the number of repeating comb units, A is the plate area, and V is the applied voltage.

The electrostatic force generated is $0.019 \mu N$ when a $10 \mu N$ force is applied. This undesired force is negligible considering the device resolution and measurement range, and can be further reduced by applying excitation signals of lower magnitude.

VI. CALIBRATION

The excitation waveform of the readout circuit is a $1MHz$ square wave nominally at $5V$. The circuit utilizes a buffer amplifier leading into a synchronous demodulator which supplies feedback to the drive voltage. Calibration was conducted using a microscale (AG285 DeltaRange). Fig. 8 shows the calibration results, and device specifications are summarized in Table 1.
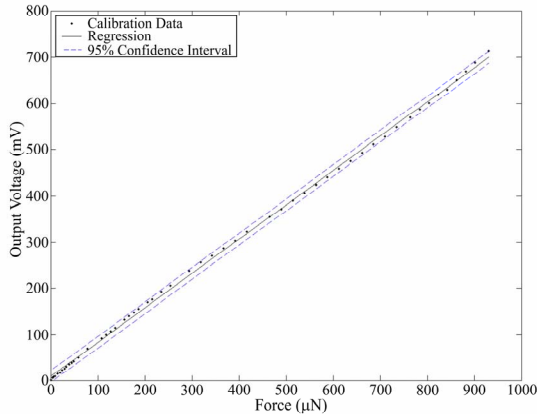

Fig. 8. Force sensor calibration results.

VII. DROSOPHILA FLIGHT FORCE MEASUREMENT

The force sensor has been applied to characterizing the flight forces produced by tethered fruit flies. Fruit flies are particularly well adapted for flight and provide an ideal model for studying the neurophysiology underlying flight control.

In the experiments, individual flies were attached to the MEMS sensor probe following the procedure described in [16]. First, the fly was immobilized on a custom machined stage cooled by a thermostat controlled Peltier element to 4°C. Second, a drop of UV sensitive glue (Loctite, Duro Clear Glass Adhesive) with an approximate diameter of $50\mu m$ was applied to the fly's thorax using a thin tungsten probe mounted on a micromanipulator (Sutter MP285). Third, the MEMS sensor probe was brought into contact with the glue, which was cured with a UV light gun (ELC305). Finally, the sensor with attached fly was lifted away from the mounting stage. After the fly's body warmed up, typically within a few minutes, the fly initiated tethered flight. Fig. 9 shows a fruit fly tethered to the force sensor probe, where the force sensor was wired bonded to a PCB.
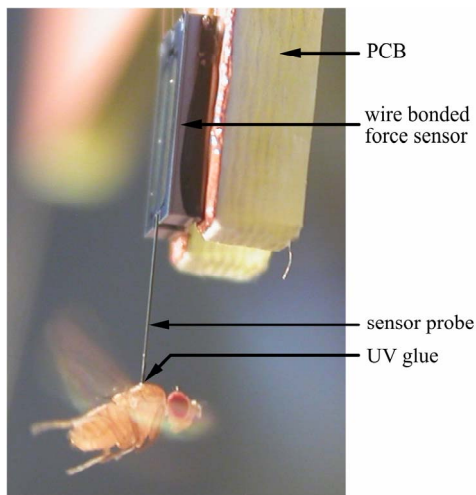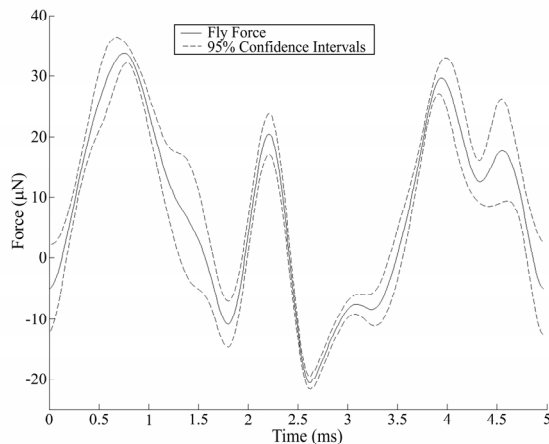
Fig. 9. Force sensing of Drosophila tethered to sensor.

Fig. 10. Drosophila flight force data of one full stroke.

Data was collected from six fruit flies at *5kHz*, and one data set is shown in Fig. 10. The measured signal is periodic, with a fundamental wing beat frequency around *200Hz*. The five local maxima and a saddle point shown in Fig. 10 indicate a higher frequency component in the force signal and considerable negative lift during parts of the stroke. This difference is most probably due to wing inertial forces, i.e., the force applied by the wings to the thorax due to their acceleration. The average lift force is 9.3μN, which is in the range of typical body weights of fruit flies. The results demonstrate the effectiveness of this technique for reliable and precise real-time measurements of flight forces in tethered flying fruit flies.

VIII. CONCLUSION

This paper presented a MEMS micro force sensor with a novel configuration of differential tri-plate comb drives suitable for bulk micromachining. The MEMS force sensor is capable of achieving previously unavailable application needs in terms of sensitivity, range, physical size, robustness, and geometry concerns. For the first time, both aerodynamic and inertial forces of Drosophila were captured in real time using a MEMS force sensor providing valuable data for understanding Drosophila's flight behavior. The future integration of the MEMS force sensors into a closed-loop flight simulator will provide a novel and efficient experimental paradigm for further insect neurophysiology studies.

IX. REFERENCES

[1]   G.M. Nelson and R.D. Quinn, "Posture control of a cockroach-like robot" *IEEE Control Systems Magazine*, Vol. 19, No. 2, pp. 9-14,1999.

[2]   J.E. Clark, J.G. Cham, S.A. Bailey, E.M. Froehlich, P.K. Nahata, R.J. Full and M.R. Cutkosky, "Biomimetic design and fabrication of a hexapedal running robot" *The IEEE International Conference on Robotics and Automation*, Seoul, Korea, May 21-26,2001,pp. 3643-3649

[3]   M.C. Birch, R.D. Quinn, G. Hahm, S.M. Phillips. B.T. Drennan, A.J. Fife, R.D. Beer, X. Yu; S.L. Garverick, S. Laksanacharoen, A.J. Pollack, and R.E. Ritzmann, "Cricket-based robots" *IEEE Robotics & Automation Magazine*, Vol. 9, No. 4, pp. 20-30, 2002

[4]   M.C. Montesi, B. Martini, A. Pellegrinetti, P. Dario, L. Lencioni and A. Montano "An SMA-based flexible active endoscope for minimal invasive surgery " *Journal of. Micromechanical. Microengineering.*, Vol. 5, pp. 180-182, 1995

[5]   M. Sitti, "Piezoelectrically actuated four-bar mechanism with two flexible links for micromechanical flying insect thorax" *IEEE/ASME Transactions on Mechatronics*, Vol. 8, No. 1, pp. 26-36, 2003

[6]   J. Yan, R. Wood, S. Avandhanula, M. Sitti and R.S. Fearing, "Towards flapping wing control for a micromechanical flying insect thorax" *The IEEE International Conference on Robotics and Automation, Seoul*, Korea, May 21-26, pp. 3901-3908, 2001,

[7]   S. Sane, "The aerodynamics of insect flight", *The Journal of Experimental Biology,* Vol. 206, pp. 4191-4208, 2003

[8]   S. Mao and J.H. Wu, "Aerodynamic force generation and power requirements in forward flight in a fruit fly with modeled wing motion", *The Journal of Experimental Biology,* Vol. 206, pp. 3065-3083, 2003

[9]   M. H. Dickinson, F. O. Lehmann, S. P. Sane, "Wing rotation and the aerodynamic basis of insect flight", *Science*, Vol. 284, 1954-1960, 1999

[10]   M. H.Dickinson, K. G. Gotz, "The wake dynamics and flight forces of the fruit fly Drosophila melanogaster"*,The Journal of Experimental Biology*, Vol. 9, pp. 2085-2104

[11] S.N. Fry, R. Sayaman, M.H. Dickinson, "The aerodynamics of free-flight maneuvers in Drosophila," *Science*, Vol. 300, pp. 495-498, 2003.

[12] W.C. Tang, T.H. Nguyen, M.W. Judy, and R.T. Howe, "Electrostatic comb drive of lateral polysilicon resonators," *Sensors and Actuators A*, Vol. 21, pp. 328-331, 1990.

[13] Yu Sun, B.J. Nelson, D.P. Potasek, and E. Enikov, "A bulk microfabricated multi-axis capacitive cellular force sensor using transverse comb drives," *Journal of Micromechanics and Microengineering (JMM)*, Vol. 12, No. 6, pp. 832-840, 2002.

[14] F. Goodenough, "Airbags boom when IC accelerometer sees 50g," *Electronic Design*, Vol. 39, pp. 45-56, 1991.

[15] J.M. Gere, *Mechanics of Materials*, 5th Edition, Pacific Grove, 2001.

[16] L.F. Tammero and M.H. Dickinson, "Collision-avoidance and landing responses are mediated by separate pathways in the fruit fly - Drosophila melanogaster," *Journal of. Experimental. Biology*, Vol. 205, pp. 2785-2798, 2002.